A98-31452

ICAS-98-1,3,2

PREDICTED DEEP-STALL FLIGHT CHARACTERISTICS OF TWO HYPERSONIC FLIGHT VEHICLES

M. R. Mendenhall* and M. C. Hegedus**
Nielsen Engineering & Research
Mountain View, CA

G. D. Budd+ and A. J. Frackowiak++
NASA Dryden Flight Research Center
Edwards, CA

ABSTRACT

An analytical investigation into the feasibility of using deep-stall flight for the return of two hypersonic configurations is described. The flight vehicles considered are the booster stages of the Pegasus XL launch vehicle and the X-34 hypersonic research vehicle. In each study, a combination of analytical and experimental longitudinal aerodynamic characteristics is used in a 3-DOF simulation to demonstrate the deep-stall flight characteristics. Both configurations exhibit stable, deep-stall flight over a wide range of Mach numbers, and they demonstrate the feasibility of a return trajectory with deep-stall flight. Flight test results are presented to validate and demonstrate the low-speed deep-stall flight characteristics of the Pegasus XL first stage.

SYMBOLS

C_A	Axial-force coefficient
C_N	Normal-force coefficient
C_m	Pitching-moment coefficient
M_∞	Mach number
α	Angle of attack
γ	Flight path angle
δ_e	Elevon deflection angle
θ	Euler angle measured from the horizontal

*Vice President, Associate Fellow AIAA
**Research Engineer, Member AIAA
+Project Manager
++Aerospace Technician

INTRODUCTION

Post-stall flight at very high angles of attack, though often considered a flight condition to be avoided at all costs, has been proposed as a means to provide a number of useful and essential benefits.[1] For example, it could possibly be used as an emergency recovery procedure for aircraft in flat spins, as a technique for increased maneuverability of modern fighter aircraft, and as a landing option for V/STOL aircraft.[2] The advantages of deep-stall flight have also been used by free-flight model aircraft enthusiasts for more than 50 years. The less desirable characteristics of deep stall have been described previously.[3,4]

It has been suggested that a deep-stall flight condition could provide a means to fly back two different hypersonic vehicles.[5] The first is the normally-expendable first-stage Pegasus XL air-launched space booster after separation of the second stage. The second is the X-34 hypersonic research vehicle. The feasibility of deep-stall flight of the two different configurations is the subject of the analysis reported herein.

The analysis of the Pegasus XL stage one will commence after burnout of the rocket motor and separation of the payload fairing portion of the vehicle forward of the wing leading edge (Fig. 1). Separation occurs at approximately Mach 8 and 150,000 feet altitude. The configuration is statically unstable without the forward part of the fuselage. The analytical investigation will focus on the possibility of trimming the vehicle at a high angle of attack with its elevons to return it to a low altitude and subsonic Mach number where a retro-rocket or parachute would arrest the near vertical descent for a soft landing.

The analysis of the X-34 flight vehicle (Fig. 2) will begin at the end of the test flight at approximately Mach 8 at 150,000 feet. altitude. Using the elevons and/or body flap for trim at a post-stall angle of attack, the vehicle will be returned to a subsonic Mach number at a low altitude where it will recover to a more conventional flight condition for a normal landing.

ANALYTICAL APPROACH

Aerodynamic Characteristics

The two configurations considered in this study are the Pegasus XL first stage and the X-34 shown in Figures 1 and 2, respectively. The CG location shown on each vehicle corresponds to the assumed mass distribution for the return flight.

Aerodynamic characteristics (C_N, C_A, and C_m) are required for $0.5 \le M_\infty \le 9$ and angle-of-attack range 0-360° to cover the entire range of possible flight conditions which may be encountered by each vehicle during the deep-stall portion of the return flight. The aerodynamic characteristics are also needed for possible control deflections. Obviously, this extensive matrix of aerodynamics is not available for these vehicles, so much effort in the current study involved the generation of adequate aerodynamics under extreme flight conditions for use in simulating the deep-stall flight characteristics.

Selected wind tunnel data are available to define the aerodynamic characteristics of the complete Pegasus XL and X-34 vehicles. Most of these data are confined to the normal test conditions; for example, $0.25 \le M_\infty \le 4.5$ at $0 \le \alpha \le 25°$. Some data are available at $M_\infty = 6$ for a limited angle of attack range. It is apparent that aerodynamic coefficients are missing for the high angles of attack of interest in this investigation. The following discussion outlines the procedures used for this initial study.

Pegasus XL. The first problem for the Pegasus XL return configuration is that this particular configuration with the nose ahead of the wing removed has never been tested in a wind tunnel nor studied analytically. The procedure used for this configuration involved a correction of the existing wind tunnel data for a complete configuration. Analytic and experimental data for the normal force and center of pressure on a nose similar to the second and third stage shape were used to correct the wind tunnel data. The pitching moments on the modified configuration were transferred to the new CG location aft of the wing. This results in aerodynamic coefficients over a limited range of flight conditions which can be used to check the analytical methods.

The next step is to identify prudent means to extrapolate these data to the higher Mach numbers, angles of attack, and elevon deflection angles required for the return mission. The elevon deflections were extrapolated linearly from $\delta_e = -30°$ in the test data to $\delta_e = -45°$. The analysis performed during this study determined the Pegasus return trajectory had the best trim characteristics at $\delta_e = -30°$; therefore, the suitability of the extrapolation to $\delta_e = -45°$ was not investigated further. Extrapolation did not seem reasonable for high angles of attack; therefore, analytical procedures were adopted. A graphical outline of the aerodynamics procedures used for Pegasus in the various flight regimes is shown in Figure 3.

The modified Pegasus XL configuration was examined at Mach numbers less than 2.0 with the code M3HAX (Ref. 6) for the flow conditions of the low Mach number wind tunnel tests. The analytical results are in good agreement with the corrected wind tunnel data. Since M3HAX is built around a high angle-of-attack wing database with analytical models for fuselage effects, it was used to calculate the aerodynamic characteristics of the Pegasus XL to $\alpha = 90°$ for $M_\infty \le 2$. For $90° \le \alpha \le 180°$, an analytical model of a tail-first Pegasus configuration was considered with M3HAX. These results were verified near $\alpha = 180°$ using alternate analytical methods.[7,8]

At Mach numbers between 2.0 and 4.6, the corrected wind tunnel data were used at the lower angles of attack to check the analytical results. At very high angles of attack approaching 90°, a modified Newtonian method with corrections from flat plate and cylinder data was used to calculate the normal force and center of pressure. A cubic spline fit between the low-angle-of-attack results and the Newtonian results was used to fill in the intermediate angles. A similar method was used to fill in the database at angles of attack greater than 90°.

Modified Newtonian methods were used for the Pegasus XL at all Mach numbers greater than 5 and all

angles of attack between 0 and 360°. It was necessary to include the full range of angles of attack because of the possibility of Pegasus tumbling immediately after separation of the payload fairing.

Selected aerodynamic results for the modified Pegasus XL configuration are shown in Figure 4. The trim angles of attack for the range of Mach numbers of interest are shown in Figure 5. Notice that the Pegasus XL trims at approximately 130-140° for supersonic Mach numbers. The trim angle drops to about 110° in subsonic flow.

X-34. Wind tunnel data are available for a model similar to the X-34 configuration shown in Figure 2, and these data were corrected to reflect small configuration changes. The experimental results were used to form the low angle aerodynamic characteristics ($\alpha < 20^{\circ}$) for Mach numbers less than 6. The normal force and center of pressure at high angles of attack were obtained from a combination of a modified Newtonian method and an estimate based on three-dimensional flat plate data from Reference 9. The latter two methods were in reasonable agreement. A spline fit between the experimental data and the high angle results provided the complete range required. A graphical outline of the procedures used in the various flight regimes is shown in Figure 6.

Selected aerodynamic results for the X-34 configuration are shown in Figure 7 for zero elevon deflection angles. The X-34 trims at about 90° angle of attack at all Mach numbers. Initial studies showed that neither positive nor negative control deflections benefit the deep-stall trim characteristics; therefore, only zero deflection cases were analyzed.

At Mach numbers 0.2 and 0.6, the C_N curves are flat between an angle of attack of 40 and 140°. This is a result of using a quadratic spline with a flat line to model the CN instead of a cubic spline model which had undesirable characteristics at these Mach numbers. This model was validated with wing-alone data for similar high angles of attack at these subsonic Mach numbers.

Some additional validation for the approach used for X-34 is available. Wind tunnel data on the Shuttle Orbiter for angles of attack up to 90 are available.[10] The analytical procedures used for X-34 were applied to the Shuttle Orbiter at supersonic Mach numbers and a wide range of angles of attack. These results are presented in Figure 8. The general character of the predicted aerodynamics is in agreement with the measurements at $\alpha = 90^{\circ}$ for supersonic Mach numbers between 2.0 and 4.6.

Trajectory Simulations

The simulation of the motion of the two vehicles in a deep-stall flight condition is accomplished with a three-degree-of-freedom equations-of-motion solver. For this preliminary analysis, the motion was restricted to the pitch plane to better understand the basic flight characteristics.

The trajectory simulator requires the mass and inertia characteristics of the vehicles and the aerodynamic characteristics (C_N, C_m, C_A) for the range of Mach numbers and angles of attack anticipated for the flight.[11] The effects of elevon deflection are included. The aerodynamic information is stored in tabular form for use by the trajectory simulator, and the initial conditions are specified for the start of the motion. The initial conditions include the speed, direction, attitude, and altitude of the vehicle. Initial rotation rates in the pitch plane are also specified.

ANALYTICAL RESULTS

Predicted trajectory characteristics were obtained for both vehicles for a variety of initial conditions to better understand the sensitivity of the solutions to starting flow parameters such as flight-path angle, angle of attack, pitch rate, and time of elevon deflection. A representative sample of the predicted results follows.

Pegasus XL

The initial simulation results of the Pegasus XL first stage are shown in Figure 9. Separation of the upper stages is assumed to occur at Mach 8 at 150,000 feet with the first stage at 0° angle of attack on a flight path 18° above the horizontal. For this first study, Pegasus was flown without control ($\delta_e = 0^{\circ}$) to observe its flight characteristics. As expected, the statically unstable configuration began to pitch up slowly into a tumbling motion. With elevons undeflected, Pegasus does not achieve trimmed flight. After more than two complete revolutions in pitch, the rotation was stopped in the simulation at t = 100 seconds (denoted as X in Figure 9), and the elevons were deflected to -30°. This

configuration has a trim angle of attack of approximately 140°, and the trajectory continued as shown in Figure 9(a). Though difficult to see in these vector plots, the Pegasus XL stage one configuration began a large-amplitude pitch oscillation around the trim angle of attack. This is more easily seen in the angle-of-attack history in Figure 9(b).

The second trajectory simulation for Pegasus XL stage one begins with a different scenario. In this case, the first stage is trimmed at $\alpha = 135°$ with $\delta_e = -30°$ immediately after separation. All other flight parameters are the same as the first case. The results of this simulation are presented in Figure 10. Notice that the altitude continues to increase as before, but the maximum altitude is significantly lower than before because of the increased drag at the trimmed attitude. The vehicle is obviously stable from Mach 8 down to Mach 0.8. Without any changes in elevon deflection, Pegasus trims at approximately 135° in supersonic flow, and the trim angle reduces to approximately 110° or less in subsonic flow as illustrated in Figure 10(c). The amplitude of the pitch oscillations in supersonic flow is only about 4°. The Mach number history is shown in Figure 10(d).

It is apparent from the second simulation that if the initial rotation of Pegasus XL can be controlled after staging and it can achieve its trimmed flight attitude, it will be stable in a deep stall condition for the remainder of the flight.

X-34

A trajectory simulation of the X-34 configuration was run with initial conditions prescribed. Assuming Mach 8 at 150,000 feet in horizontal flight, the X-34 is pitched to 90° angle of attack and trimmed with no deflections of the body flap or elevons. The results are shown in Figure 11. X-34 trims at angles of attack between 90 and 100° over most of the flight range, and it is stable. The small pitch oscillations shown in Figure 11(b) are indicative of the level of stability of this vehicle in a deep-stall configuration.

Notice that the Mach number history in Figure 11(c) is much different than that of the Pegasus XL discussed above. One reason is the initial flight path angle. Since its mission is different from Pegasus, X-34 was assumed to be in horizontal flight initially. This does not result in any altitude increase; therefore, the dynamic pressure does not decrease and the drag stays very high, resulting in the rapid decrease in Mach number.

INITIAL FLIGHT TESTS

An unpowered, uninstrumented, free-flying 5.2% scale drop model of stage one of the Pegasus XL launch vehicle (Fig. 12) was constructed and flight tested at high-angle-of-attack deep-stall conditions at the NASA Dryden Flight Research Center. Elevon deflections tested were -30°, -45°, and -60° (leading edge down for all cases). The center of gravity (CG) was located at the representative longitudinal CG position for a spent Pegasus XL first stage booster. No attempt was made to properly scale the vehicle's inertial properties. The model weighed 5.75 ounces, and was constructed from balsa wood, paper, and foam.

The model was dropped from approximately 400 feet, yielding flight durations of approximately 20 seconds, depending on the vehicle configuration tested. No recovery system was utilized due to the small size and light weight of the test model. The flights were conducted on a cool day with light surface winds and no perceivable turbulence. All of the flights were recorded on video tape.

Upon release from the carrier "mother ship," the drop model tumbled for a few seconds before stabilizing in an upright, slightly nose high attitude in a near vertical, tail first descent. A review of the flights on video tape indicates that the flight path angle is approximately 100° to 135°, depending on the elevon deflection chosen.

The model exhibited varying degrees of pitch and roll stability during the descents flown. All configurations tested exhibited tail-first gliding flight, with a pronounced nose high attitude. Increasing the preset elevon deflection yielded an increase in the trim pitch attitude.

Flights with the elevon deflection set to -45° were the most stable in both the pitch and roll axes. Little or no motion in any axis was noted once the model entered the deep-stall descent. Flights with the elevons set to -60°exhibited less pitch and roll stability, with a mild, but stable, wing rock. With the elevons set to -30° at drop, the vehicle began a lateral wing rock buildup that

eventually diverged into a complete roll. Then, the model restabilized in an upright attitude and began the wing rock buildup again. The model showed no significant change in pitch attitude during this lateral maneuver.

CONCLUSIONS

Deep-stall flight appears to be feasible with both the Pegasus XL stage one and X-34 vehicles if they can be trimmed at an early time after rocket motor burnout. Trimmed flight must be achieved before the pitch rotational motion builds up to a level which is difficult or impossible to damp out. The Pegasus trims at a much higher angle of attack than the X-34, though the trim angle does decrease at subsonic speeds.

If this fly-back procedure is pursued further, wind tunnel tests at high angles of attack and a range of Mach numbers are required to better define the aerodynamic characteristics for the simulations. Even if the entire aerodynamic matrix is not obtained with testing, sufficient data are required to sanity check the predictions and calibrate the prediction methods so that the aerodynamic characteristics can be obtained analytically.

The trajectory simulations should be expanded to six degrees of freedom to include lateral characteristics. The yaw and roll characteristics of these vehicles may be important during the entry into deep-stall flight and should be considered in a future investigation.

Finally, additional flight tests of models and full-scale vehicles is the best way to validate the concept of deep-stall return.

REFERENCES

1. Sim, A. G.: Flight Characteristics of a Modified Schweizer SGS 1-36 Sailplane at Low and Very High Angles of Attack. NASA Technical Paper 3022, July 1990.

2. Strom, T. H. and Alford, W. J., Jr.: Controllable Supernormal Flight: A Future Possibility. SAE Paper 821469, 1982.

3. Polhamus, E. C.: The Deep-Stall Problem of T-Tail Aircraft. *Space/Aeronautics*, May 1966, pp. 106-8.

4. Lina, L. J. and Moul, M. T.: A Simulator Study of T-Tail Aircraft in Deep Stall Conditions. NASA TM X-56806, 1965.

5. Mendenhall, M. R., Hegedus, M. C., and Love, J. F.: Aerodynamic Analysis of the Deep-Stall Flight Characteristics of the Pegasus XL and X-34 Configurations. NEAR TR 516, December 1996.

6. Lesieutre, D. J., Love, J. F., and Dillenius, M. F. E.: M3HAX Aerodynamic Analysis for Finned Vehicles with Axisymmetric Bodies. NEAR TR 493-D, November 1996.

7. Dillenius, M. F. E., Perkins, S. C., Jr., and Lesieutre, D. J.: Modified NWCDM-NSTRN and Supersonic Store Separation Programs for Calculating NASTRAN Forces Acting on Missiles Attached to Supersonic Aircraft. NWC TP 6834, 1986.

8. Lesieutre, D. J., Dillenius, M. F. E., and Whittaker, C. H.: Program SUBSAL and Modified Subsonic Store Separation Program for Calculating NASTRAN Forces Acting on Missiles Attached to Subsonic Aircraft. NAWCWDNS TM 7319, May 1992.

9. Hoerner, S. F.: Fluid Dynamic Drag. Published by the author, 1958.

10. Spencer, B., Jr., and Calloway, R. L.: Supersonic Aerodynamic Characteristics of a Space Shuttle Orbiter Model at Angles of Attack from 20° to 90°. NASA TM 89112, July 1987.

11. Dillenius, M. F. E., Love, J. F., Hegedus, M. C., and Lesieutre, D. J.: Program STRLNCH for Simulating Missile Launch from a Maneuvering Parent Aircraft at Subsonic Speeds. NEAR TR 509, October 1996.

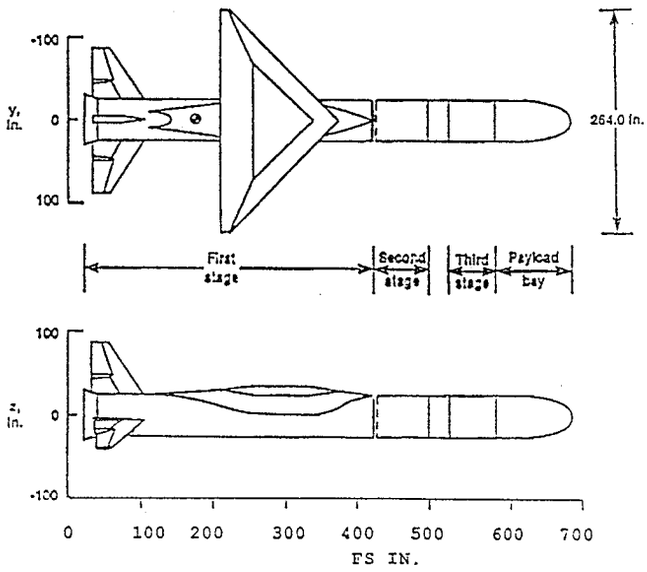

FIGURE 1 - Pegasus XL configuration.

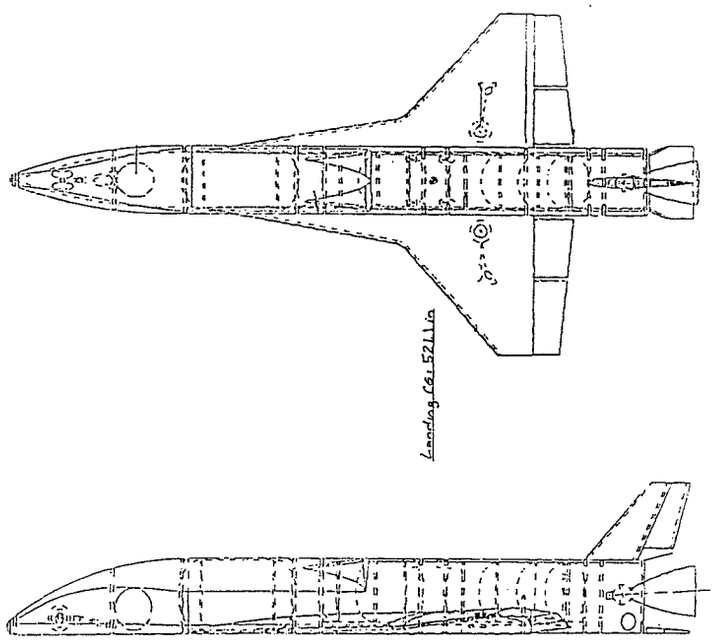

FIGURE 2 - X-34 configuration.

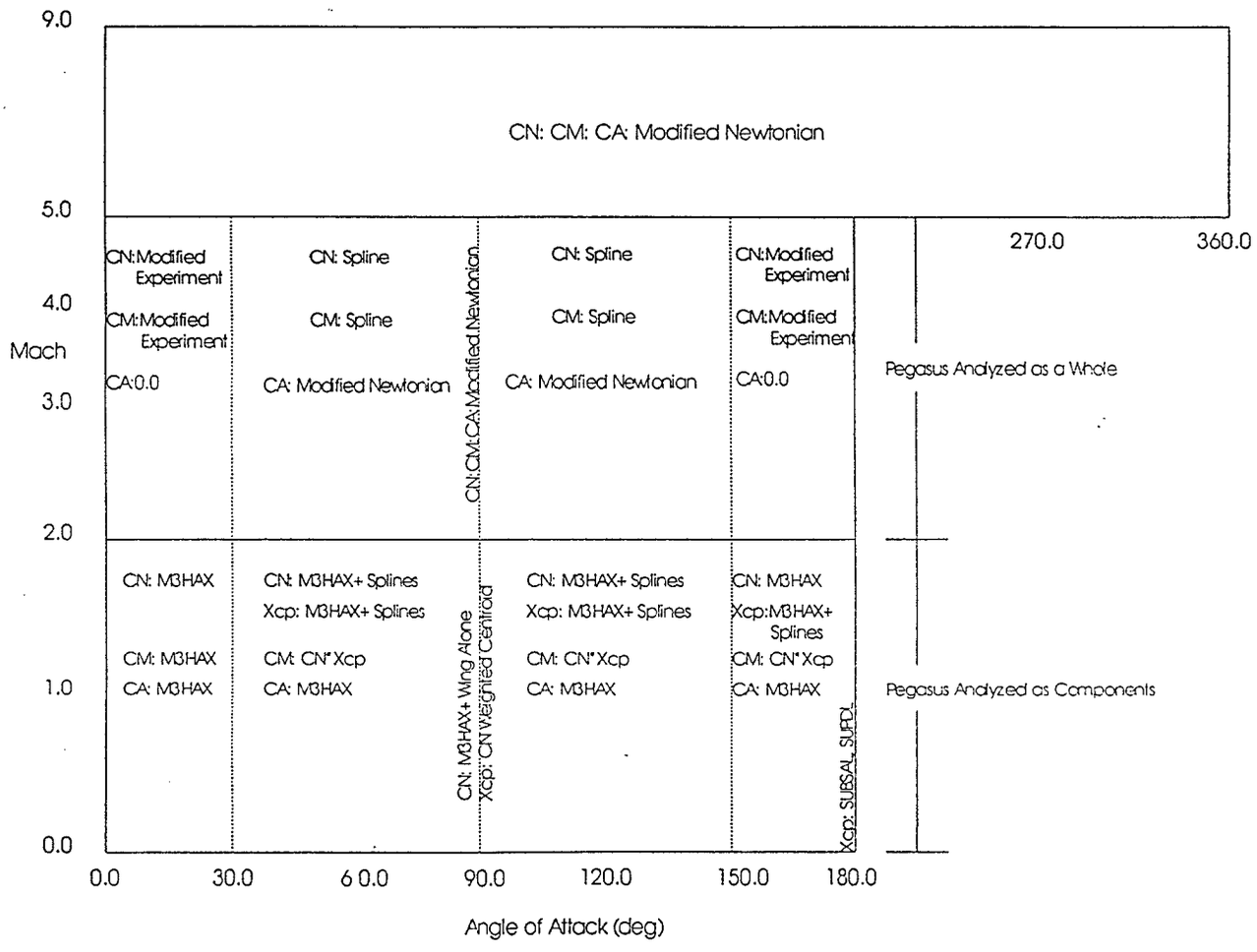

FIGURE 3 - Pegasus XL stage one aerodynamic estimation procedure.

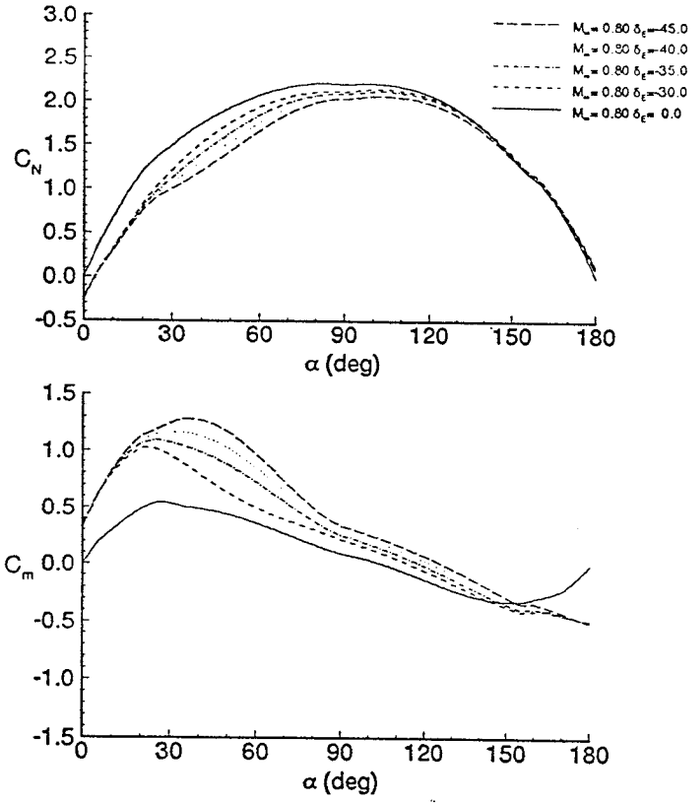

FIGURE 4 - Pegasus XL stage one aerodynamics.
(a) Mach 0.8

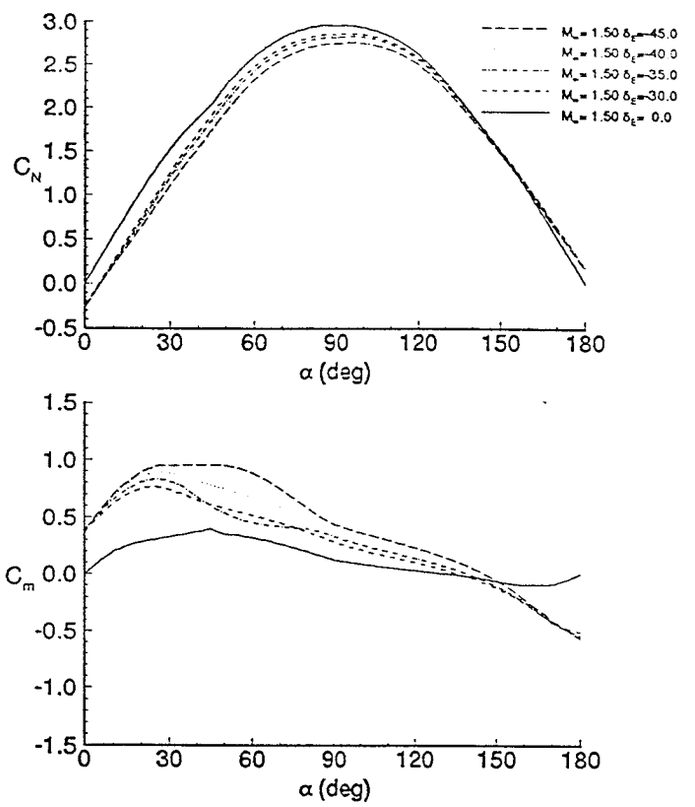

FIGURE 4 - Continued.
(b) Mach 1.5

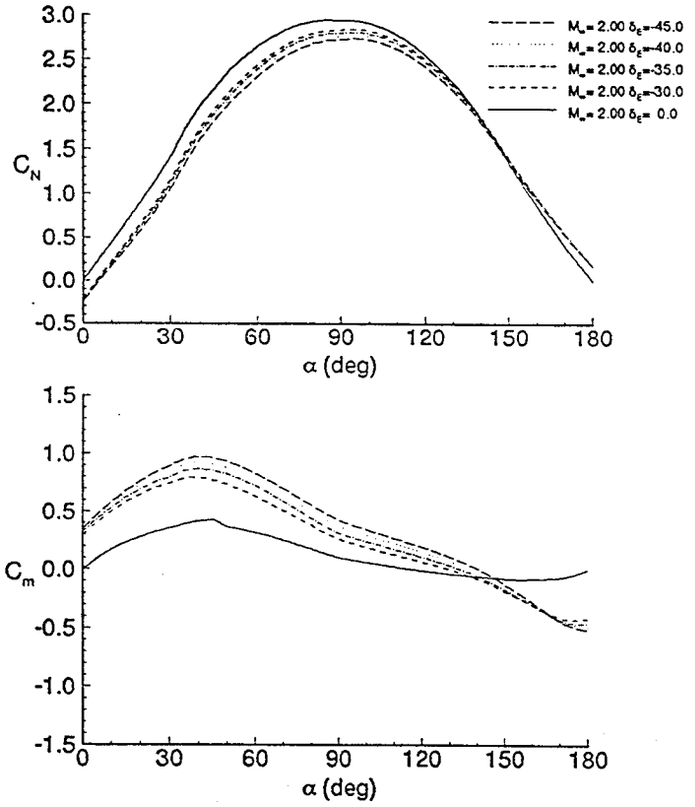

FIGURE 4 - Continued.
(c) Mach 2.0

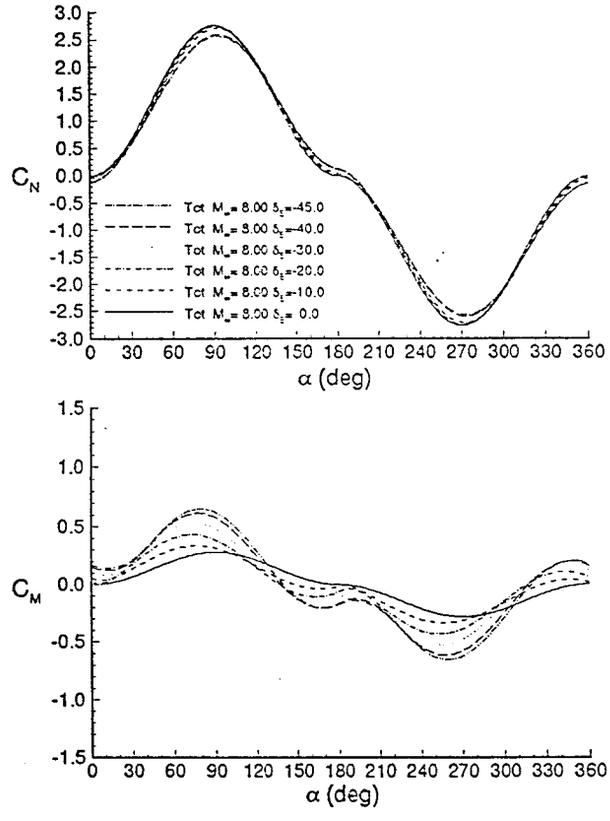

FIGURE 4 - Concluded.
(d) Mach 8.0

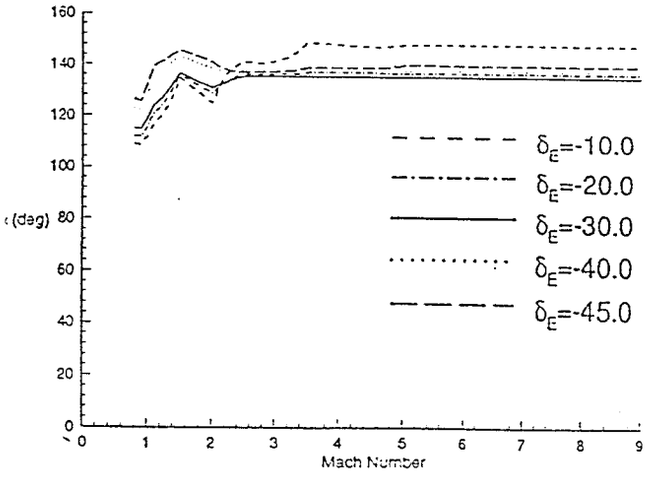

FIGURE 5 - Pegasus XL stage one trim angle of attack.

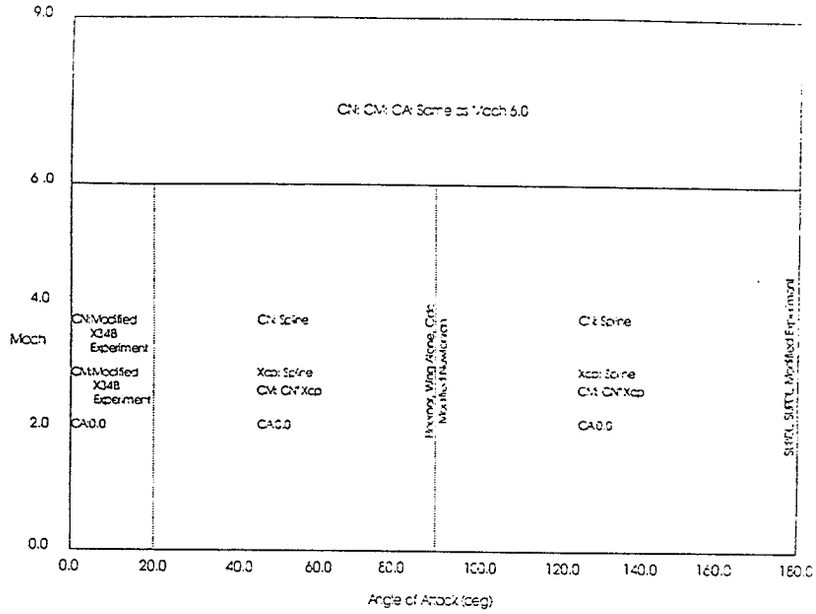

FIGURE 6 - X-34 aerodynamic estimation procedure.

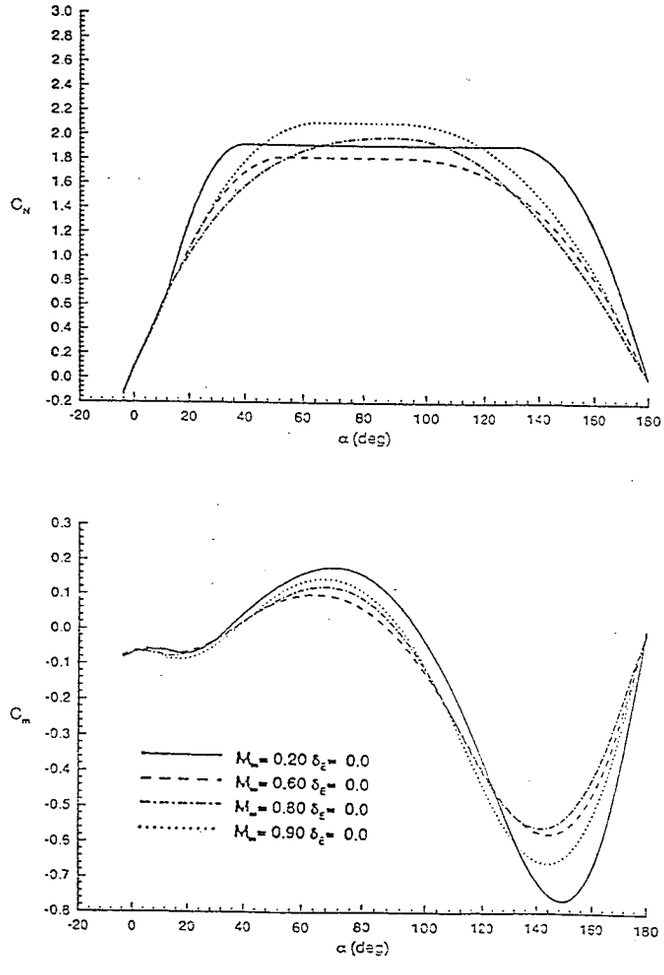

FIGURE 7 - X-34 longitudinal aerodynamics, $\delta_e = 0°$.
(a) Subsonic

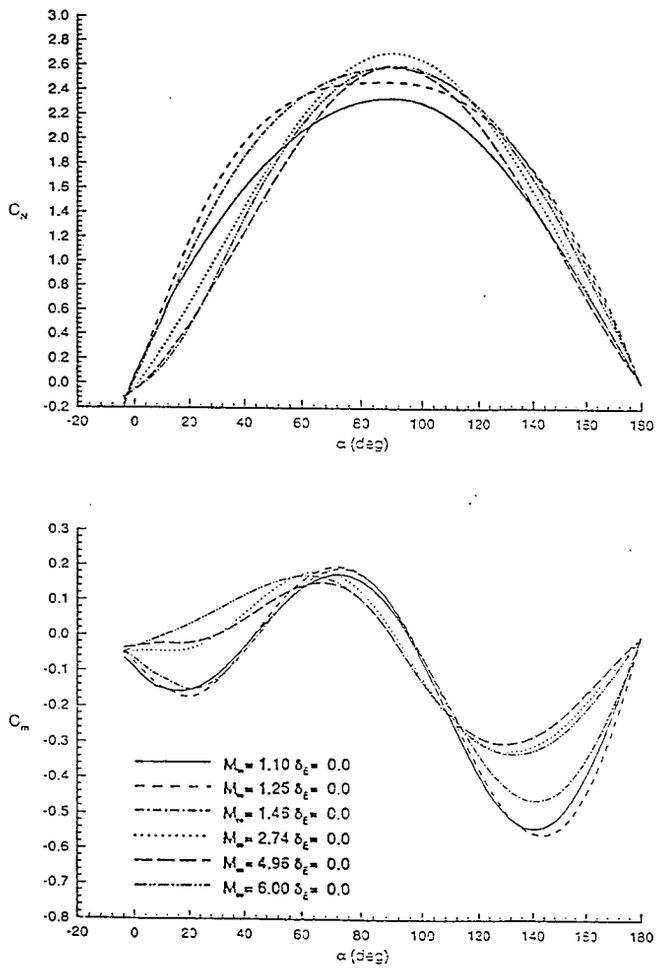

FIGURE 7 - Concluded.
(b) Supersonic

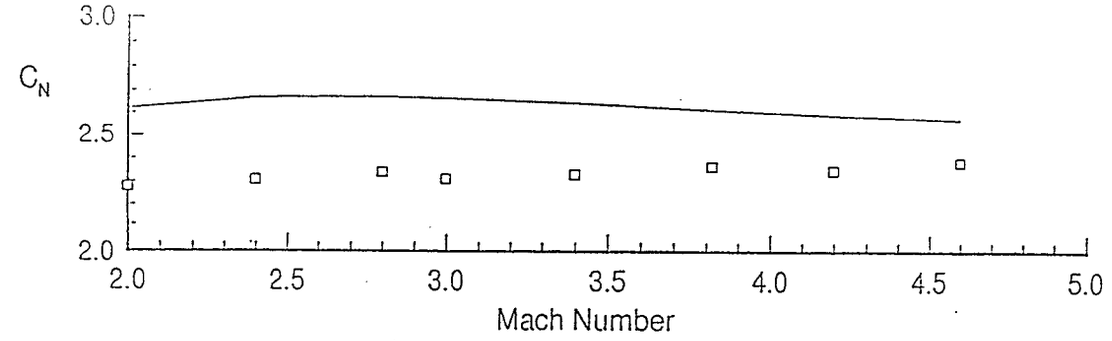

(a) Normal force coefficient

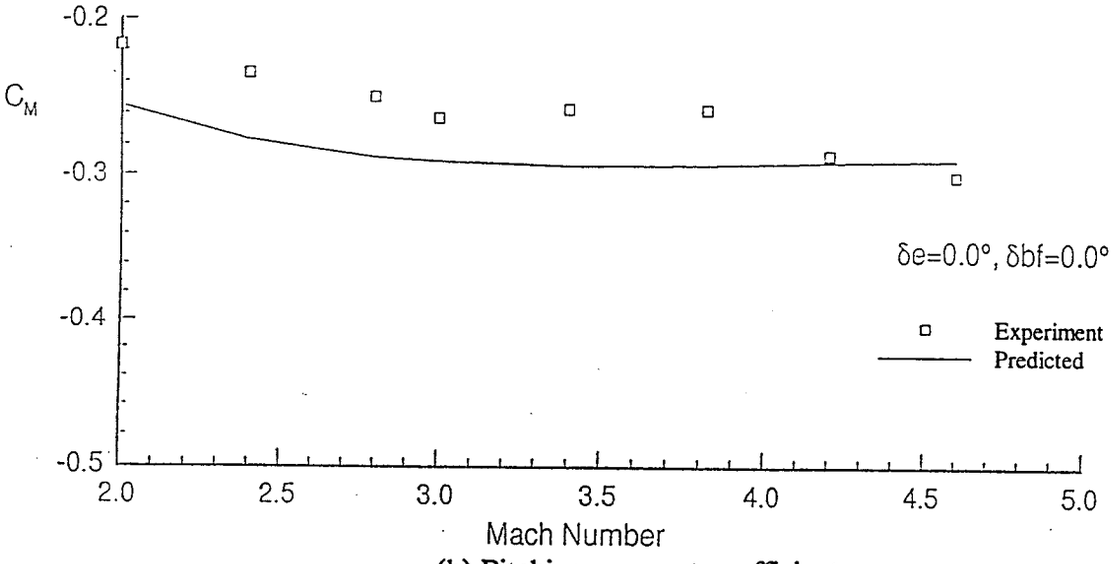

(b) Pitching moment coefficient

FIGURE 8 - Measured and predicted Shuttle Orbiter longitudinal aerodynamic characteristics, $\alpha = 90°$, $\delta_e = 0°$.

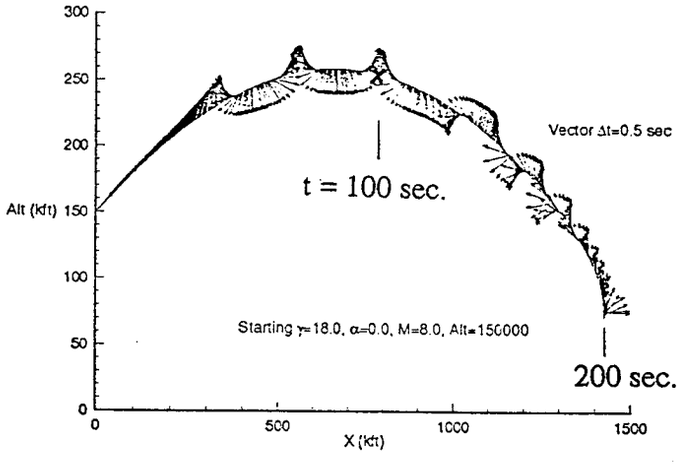

FIGURE 9 - Pegasus XL stage one deep-stall trajectory.
(a) Trajectory profile

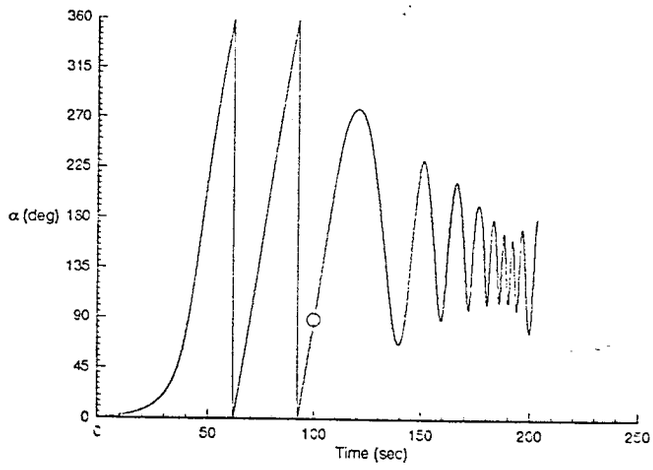

FIGURE 9 - Concluded.
(b) Angle of attack

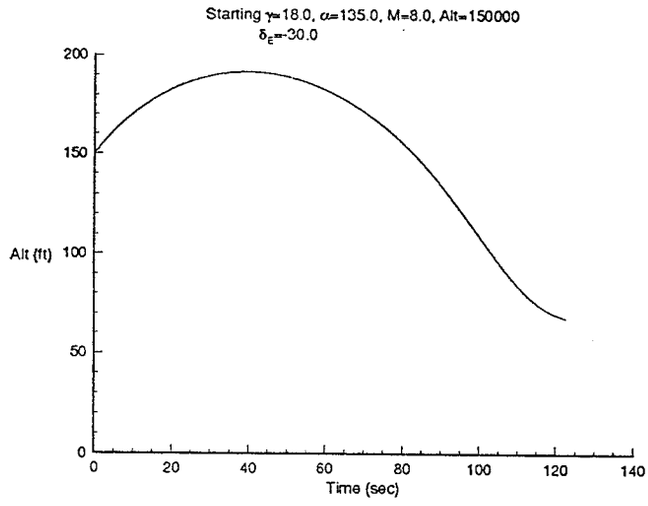

FIGURE 10 - Pegasus XL stage one deep-stall trajectory
(a) Trajectory profile

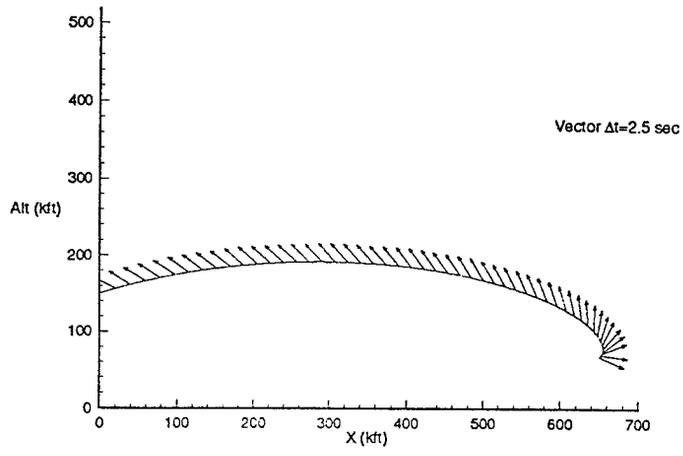

FIGURE 10 - Continued.
(b) Vehicle attitude

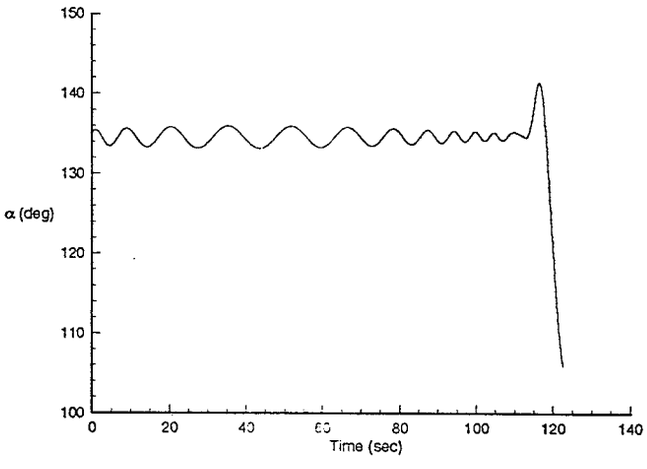

FIGURE 10 - Continued.
(c) Angle of attack

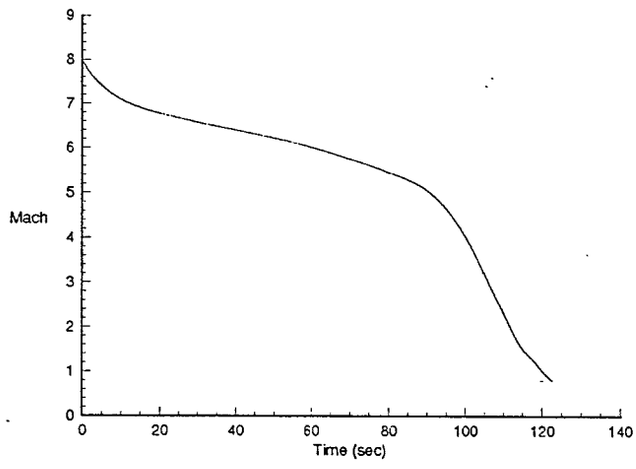

FIGURE 10 - Concluded.
(d) Mach number

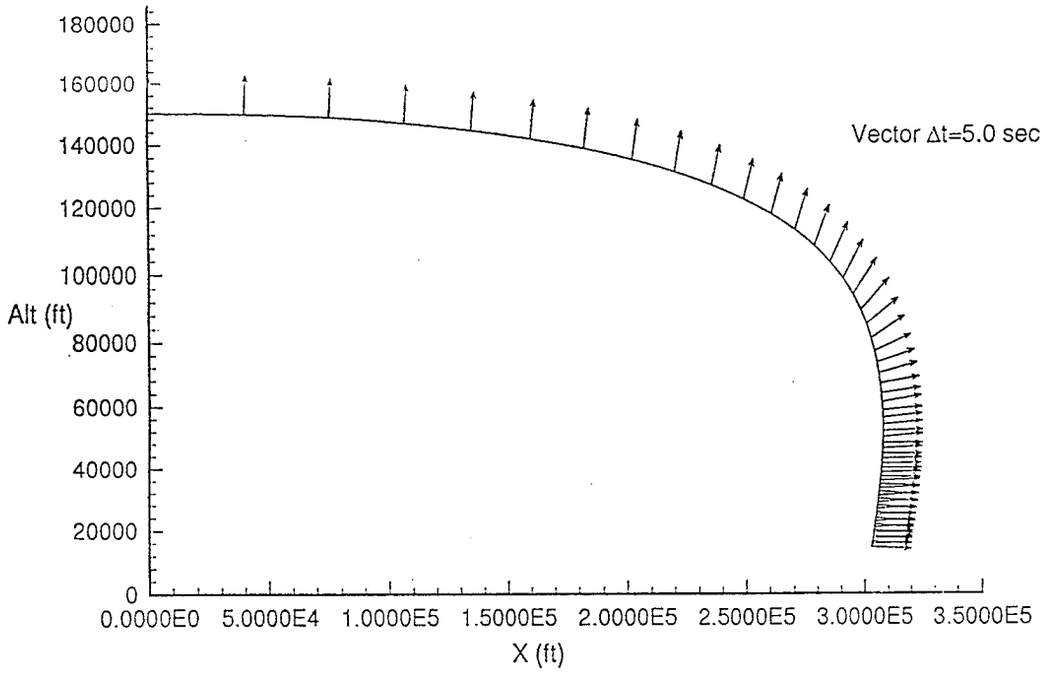

FIGURE 11 - X-34 deep-stall trajectory, trim at burn out.
(a) Trajectory profile

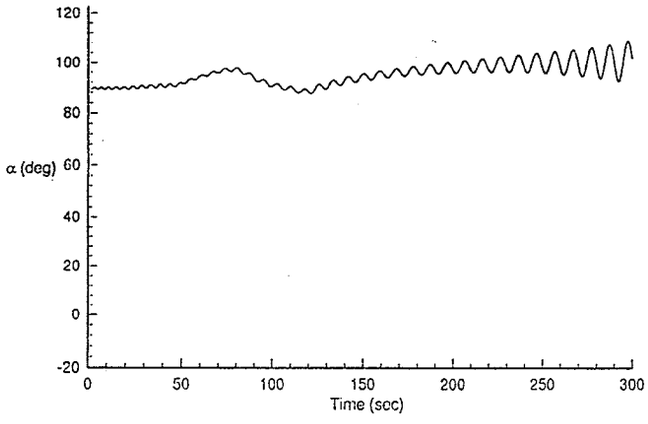

FIGURE 11 - Continued.
(b) Angle of attack

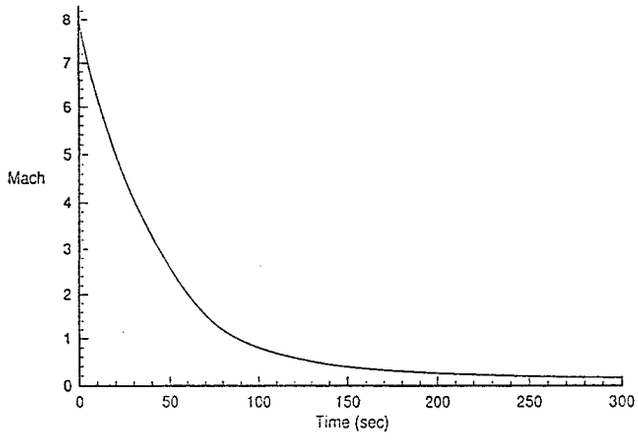

FIGURE 11 - Concluded.
(c) Mach number

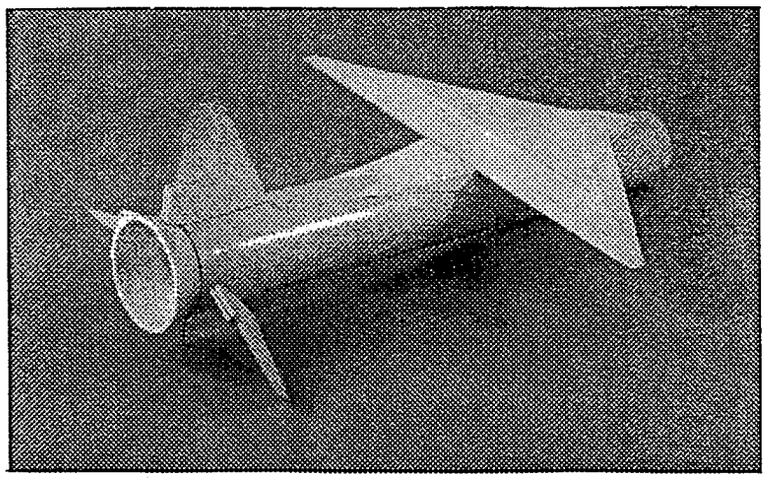

FIGURE 12 - Pegasus XL stage one low-speed drop test model.